IRON FEATURES IN THE *XMM-NEWTON* SPECTRUM OF NGC 4151

N.J. Schurch[1], R.S. Warwick[1], R.E. Griffiths[2], and A.F. Ptak[2]

[1]Department of Physics and Astronomy, University of Leicester, University Road, Leicester, LE1 7RH
[2]Department of Physics, Carnegie Mellon University, 5000 Forbes Avenue, Pittsburgh, PA 15213

Abstract

We present a detailed analysis of the hard X-ray (>2.5 keV) EPIC spectra from the first observations of NGC 4151 made by *XMM-Newton*. We fit the spectra with a model consisting of a power-law continuum modified by line-of-sight absorption (arising in both partially photoionized and neutral gas) plus additional iron-K emission and absorption features. This model provides an excellent overall fit to the EPIC spectra. The iron Kα line is well modelled as a narrow Gaussian component. In contrast to several earlier studies based on data from ASCA, a relativistically broadened iron Kα emission feature is not required by the *XMM-Newton* data. The upper limit on the flux contained in any additional broad line is $\sim$8% of that in the narrow line. The measured intrinsic line width ($\sigma = 32 \pm 7$ eV) may be ascribed to (i) the doublet nature of the iron Kα line and (ii) emission from low ionization states of iron, ranging from neutral up to FeXVII. The additional iron absorption edge arises in cool material and implies a factor ~ 2 overabundance of iron in this component.

Key words: Missions: *XMM-Newton*– Galaxies: Active – Galaxies: Seyfert – X-rays: Galaxies – Galaxies: NGC 4151

1. Introduction

The Seyfert 1 galaxy NGC 4151 is one of the brightest Active Galactic Nuclei (hereafter AGN) accessible in the X-ray band, and has been extensively studied by all major X-ray missions. This observational focus has revealed the X-ray spectrum of NGC 4151 to be a complex mixture of emission and absorption components, originating at a variety of locations from the innermost parts of the putative accretion disk, out to the extended narrow-line region of the galaxy. The X-ray spectrum emanating from the active nucleus is dominated by an intrinsic X-ray to γ-ray continuum that appears to be produced by the thermal Comptonization of soft seed photons (e.g. Haardt & Maraschi 1991; Zdziarski et al. 1994, Zdziarski et al. 1996, Zdziarski et al. 2000; Petrucci et al. 2000), plus additional contributions from reprocessing in the form of Compton-reflection and features associated with neutral iron (*e.g.* iron-K fluorescence and a neutral iron edge). Below ~ 5 keV the hard continuum is strongly cut-off by photoelectric absorption in a substantial ($N_H \sim 10^{23}$ cm^{-2}) line-of-sight gas column density (e.g. Holt et al. 1980; Yaqoob et al. 1993; Weaver et al. 1994a, Weaver et al. 1994b).

Some earlier studies based on *ASCA* observations have concluded that the line profile is complex, and is composed of with an intrinsically narrow component (Weaver et al. 1994b; Zdziarski et al. 1994, etc) plus a relativistically broadened line feature (*e.g.* Yaqoob et al. 1993; Wang et al. 2001). Furthermore the broad line profile was reported to be variable on timescales of 10^4s, corresponding to an emitting region of <0.02 AU, suggestive of an origin close to the supermassive black hole presumably in the inner regions of a putative accretion disk.

In this paper we focus on the iron-K features present in the very high signal-to-noise EPIC spectra of NGC 4151. Our analysis is based on the spectral "template" model, developed by Schurch & Warwick (2002) to interpret earlier *ASCA* and *BeppoSAX* observations.

2. The *XMM-Newton* observations

NGC 4151 was observed with *XMM-Newton* three times during the 21st and 22nd of December, 2000 (orbit 190). NGC 4151 was positioned on-axis in both the EPIC MOS and PN cameras (Turner et al. 2001; Strüder et al. 2001) with the medium filter in place. Of the three EPIC observations, one ($\sim$33 ks) was performed with the MOS and PN in small window mode, whilst the remaining two observations ($\sim$63 and $\sim$23 ks) were operated in full window mode for both instruments. The recorded events were screened with the latest available release of the *XMM-Newton* Science Analysis Software (SAS) to remove known hot pixels and other data flagged as bad. The data were processed using the latest CCD gain values and only X-ray events corresponding to patterns 0–12 in the MOS cameras and 0–4 in the PN camera were accepted. Investigation of the full field count-rate for all three observations revealed a single flaring event during the first observation. This flaring event was screened from the data, resulting in effective total exposure times of 110 ks and 91 ks respectively for the MOS and PN instruments. An investigation into the impact of pile-up on the observation showed that the effect was negligible in all the observations, largely due to the relatively faint nature of NGC 4151 during this period.

A source and background lightcurve were extracted from each individual, screened observation. These lightcurves revealed that NGC 4151 remained remarkably constant (to within 10%) for the duration of the observations, allowing us to analyse the *XMM-Newton* data without being overly concerned with the considerable spectral variability that characterized the previous *ASCA* "long-look" observation (Schurch & Warwick 2002). Source and background spectra were extracted from the same regions as the lightcurves. The spectra from the two full window mode observations were co-added to produce a single source spectrum and a single background spectrum for each instrument. The spectra were binned to a minimum of 20 counts per spectral channel, in order to apply χ^2 minimisation techniques. Here we consider only the 2.5-12 keV spectrum.

3. The spectral analysis

3.1. The initial spectral template model

We adopt the spectral template model described by, Schurch & Warwick (2002) which includes the following emission components:

1. A power-law continuum with a normalization, A_1, and photon index, Γ, exhibiting a high-energy break at 100 keV;
2. A neutral Compton-reflection component (modelled by PEXRAV in XSPEC, Magdziarz & Zdziarski 1995) with only the reflection scaling factor, R, as a free parameter. The parameters relating to the incident continuum were tied to those of the hard power-law component. In addition $\cos i$ was fixed at 0.5 and the metal abundance in the reflector was fixed at the solar value;
3. An iron Kα emission line of intensity $I_{K\alpha}$ at an energy $E_{K\alpha}$ with an intrinsic line width $\sigma_{K\alpha}$.

The complex absorber is represented as the product of two absorption components, namely a warm column density $N_{H,warm}$ and a cold gas column $N_{H,cold}$. For further details of the photoionization modelling see Schurch & Warwick (2002) and Griffiths et al. (1998). The adopted spectral model includes absorption arising in the line-of-sight column density through our own Galaxy, applied to all three emission components ($N_{H,Gal}= 2\times10^{20}$ cm^{-2}).

3.2. The spectral fitting

The template spectral model was fit simultaneously to both the small window mode and the co-added, large window mode EPIC spectra. The initial model allowed the continuum and reflection normalizations, the line properties (centroid energy, width and normalization) and the ionization parameter of the warm absorbing column to be free parameters. The values for all the remaining model parameters were set at those used in Schurch & Warwick (2002). The spectra, along with the spectral template

Table 1. Best-fit spectral model parameters

Model Parameter	Model 1	Model 2
R	$0.58^{+0.02}_{-0.06}$	$0.62^{+0.03}_{-0.06}$
$\log(\xi)$	$2.631^{+0.007}_{-0.004}$	$2.627^{+0.003}_{-0.007}$
A_{pl} [a]	$1.27^{+0.03}_{-0.01}$	$1.28^{+0.03}_{-0.02}$
$E_{K\alpha}$ [b]	$6.373^{+0.03}_{-0.02}$	$6.393^{+0.003}_{-0.002}$
$\sigma_{K\alpha}$ [b]	$0.032^{+0.07}_{-0.07}$	$0.032^{+0.005}_{-0.002}$
$I_{K\alpha}$ [c]	$1.31^{+0.3}_{-0.3}$	$1.26^{+0.03}_{-0.03}$
$E_{K,Edge}$ [b]	-	$7.13^{+0.04}_{-0.03}$
$\tau_{K,Edge}$	-	$0.11^{+0.012}_{-0.015}$
χ^2	5471.3	5297.7
d-o-f	4971	4969

[a] 10^{-2} photon keV^{-1} cm^{-2} s^{-1} [b] keV
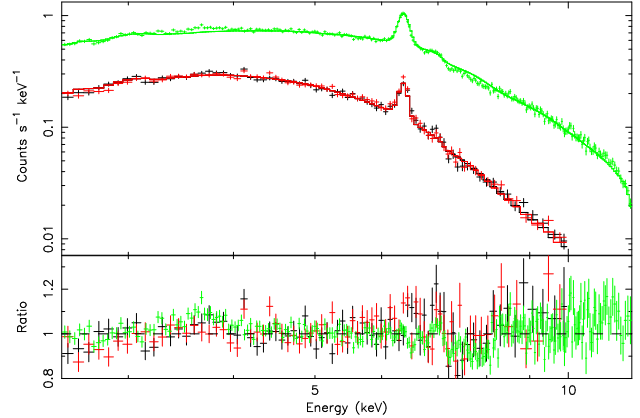[c] 10^{-4} photon cm^{-2} s^{-1}

Figure 1. The XMM-Newton EPIC spectra of NGC 4151 and the spectral template model. The MOS data, shown here in black (MOS 1) and red (MOS 2), are from the small window mode observation. The PN data, shown here in green, is from the Full Window mode co-added observation.

model fit, is shown Figure 1 and the best-fit parameters are given in Table 1, Model 1. The quoted errors (here as elsewhere in this paper) are at the 90% confidence level as defined by a $\Delta\chi^2=2.71$ criterion (*i.e.*, assuming one interesting parameter). This model gave an acceptable fit to the spectrum ($\chi^2=5465$ for 4973 d.o.f), although the data/model residuals suggest an over-prediction of the flux between 7 and 8 keV. A closer inspection of the shape of the data in this region reveals a sharp drop at ~7 keV, which we interpret as an absorption edge from neutral iron. Including an additional edge in our model, with the edge energy and the optical depth a free parameters, improved the fit dramatically ($\Delta\chi^2=173$ for 2 d.o.f; Figure 2). The best-fit parameters for the model incorporating an additional edge are given in Table 1, Model 2.

Including a further contribution to the iron Kα line profile from a broad (σ=0.2 keV) component does not improve the model fit, and sets an upper limit on the flux in the broad component of 1.0×10^{-5} photons cm^{-2} s^{-1}. Replacing the Gaussian line in the best-fit model with the
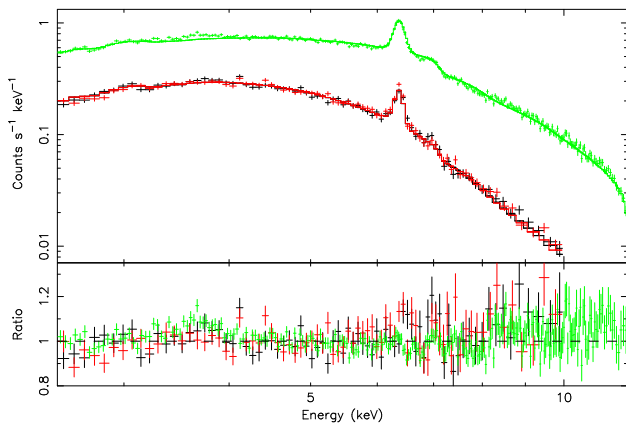
Figure 2. The XMM-Newton EPIC spectra of NGC 4151 fit with the modified spectral template model. The EPIC spectra, MOS 1 (black), MOS 2 (red) and PN (green), are fit with the spectral template model plus an additional edge feature from neutral iron at 7.1 keV.

broad emission from an accretion disk (**disk-line** model in XSPEC, Fabian et al. 1989) results in a similar fit to that for a narrow line (χ^2=5309 for 4970 d.o.f). However, in this case the derived inner radius of the accretion disk, r_i, $\sim$1000r_g gives a disk-line profile that closely resembles the observed narrow line.

4. DISCUSSION

The hard X-ray spectrum of NGC 4151 is well modelled by the spectral template model developed in Schurch & Warwick (2002), with surprisingly few modifications. In the *XMM-Newton* observations NGC 4151 was in a relatively faint state as judged against previous extensive monitoring of the source by missions such as *EXOSAT* and *Ginga*. The continuum is $\sim$60% weaker, than the faintest level measured during earlier *BeppoSAX* and *ASCA* observations, whereas the level of the Compton reflection component is $\sim$60% stronger. The ionization parameter of the warm absorber falls within the range of ionization states recorded during the *ASCA* long-look observation (ξ=2.48–2.65).

4.1. THE NATURE OF THE IRON LINE

Following the analysis described in Schurch & Warwick (2002), we model the iron Kα line in the *XMM-Newton* spectra with a simple Gaussian model at an energy corresponding to fluorescence of cold, neutral iron. The data are well modelled by this line profile and we find no evidence for the presence of a relativistically broadened iron Kα line. This is in contrast with some previous claims (Yaqoob et al. 1995; Wang et al. 2001) based on the analysis of *ASCA* observations. However, we note that further analysis of these earlier data by Schurch & Warwick (2002) *do not* require the presence of a broad line. Including a broad line in our modelling gives no statistical improve-

ment of the fit and results in an upper limit on the flux in the broad component of $\sim$8% of that in the narrow component. Modelling the line profile with a relativistically broadened disk-line profile with parameters values as quoted in Yaqoob et al. (1995) results in a poor fit to the data (χ^2=8800 for 4971 d.o.f). Similarly, modelling the line profile with the parameters quoted by Wang et al. (2001) also results in a poor fit to the data (χ^2=9438 for 4971 d.o.f). In fact the broad line profiles proposed by Wang et al. and Yaqoob et al. are both ruled out at $\gg$99.99% significance.

The measured flux in the narrow iron Kα line is $1.26^{+0.03}_{-0.03}\times 10^{-4}$ photons cm^{-2} s^{-1}, significantly lower (at $\gg 4\sigma$) than that measured in the *ASCA*, *BeppoSAX* and *Ginga* observations where the line flux was more typically $2.2^{+0.2}_{-0.3}\times 10^{-4}$ photons cm^{-2} s^{-1}; (Schurch & Warwick 2002, Yaqoob & Warwick 1991) the present measurment is also somewhat lower than the line flux reported in more recent *Chandra* observations (1.8×10^{-4} photons cm^{-2} s^{-1}; Ogle et al. 2000), implying a possible decrease in the line flux over a period of $\sim$1 year.

XMM-Newton measures a line width of 32^{+7}_{-7} eV, somewhat greater than the line width measured by *Chandra* ($\sim$5 eV). Possible explanations for the non-zero intrinsic width of the Gaussian profile include: (i) the signature of the doublet nature of the underlying iron Kα line and (ii) emission from low ionization states of iron, ranging up to FeXVII, present in the warm absorber. However, modelling the line in *XMM-Newton* with two intrinsically narrow components to represent the iron Kα doublet yields a marginally worse fit to the data (χ^2=5320 for 4970 d.o.f). The lines were fixed at the correct rest energies of the Kα_1 (6.392 keV) and Kα_2 (6.405 keV) lines and the branching ratio was fixed at the theoretical value of 1:2 respectively. We note that Ogle et al. (2000) find no evidence for Doppler broadening from their spectra.

4.2. THE IRON EDGE - A CLUE TO IRON ABUNDANCE.

The spectral model developed in Schurch & Warwick (2002) includes iron edge features from both the neutral and warm absorbers and from the Compton reflection of neutral gas, assuming in each case solar metal abundances. These solar abundance edges are insufficient to model the 7–8 keV region of the *XMM-Newton* spectrum, prompting the inclusion of an additional edge. The derived edge energy is consistant with absorption by neutral iron. This feature can be interpreted either as a result of abundance gradients or as a result of a general overabundance of iron in the absorbing material. Previous analyses of NGC 4151, albeit using a partial covering model, have also reported evidence for an overabundance of iron in NGC 4151. Yaqoob et al. (1993) quote a canonical value of A_{Fe} $\sim$2.5 times solar, based on the average of many measurements. Interpreting the additional edge required by the *XMM-Newton* data as an overabundance of iron in

the neutral absorber (Morrison & McCammon 1983), the optical depth of the edge leads to a value for the iron abundance, A_{Fe}, of $3.6^{+2.15}_{-1.8}$ times solar. Alternativly, allowing the iron abundance of the Compton reflection component to replace the additional edge in the model results in an more modest iron overabundance ($A_{Fe} \sim 2.3$), consistent with the results of Yaqoob et al. (1993), however in this case the fit becomes somewhat worse above 8 keV. If we allow an overabundance in both the neutral absorption and in the neutral reflection component, a value of $A_{Fe} \sim 2$ is required.

5. The Conclusions

Remarkably, the hard X-ray (2.5–10 keV) EPIC spectra from the recent *XMM-Newton* observation of NGC 4151 are extremely well modelled by the model developed in Schurch & Warwick (2002) with only minor modifications. The success of this simple model in modelling both previous and current data supports that the spectral variability exhibited by NGC 4151 is the product of rather subtle changes, specifically in the ionisation state of the majority of the line of sight warm absorber. The parameters of the warm absorber fit to the *XMM-Newton* data are consistent with the results from the spectral analysis of the past seven years of *ASCA* and *BeppoSAX* observations.

The chief modification to the template spectral model (Schurch & Warwick 2002) is the addition of an edge feature from neutral iron. Interpreting the edge as the result of an overabundance of iron in the cold absorber and cold reflector, then a value of $A_{Fe} \sim 2$ is required.

This analysis finds no requirement for a relativistically broadened iron Kα line feature in the *XMM-Newton* data. The upper limit on the possible flux present in any additional broad line is $\sim 8\%$ of that in the narrow line component. There is evidence that the line flux in NGC 4151 has decreased recently, possibly due to the fact that the source has been fainter during the last few years than was previously observed. The low luminosity ($L_{X,2-10} \sim 2\times10^{42}$ erg s^{-1}) of the current observation is consistent with this view.

The intrinsic non-zero width of the best-fit Gaussian line profile is suggestive of a further level of complexity to the iron Kα line feature, with possible explanations for the non-zero intrinsic width including: (i) the signature of the doublet nature of the iron Kα line, (ii) emission from low ionization states of iron, ranging up to FeXVII, present in the warm absorber.

References

Fabian A. C., Rees M. J., Stella L., White N. E., 1989, MNRAS, 238, 729.

Griffiths R. G., Warwick R. S., Georgantopoulos I., Done C., Smith D. A, 1998, MNRAS, 298, 1159

Haardt F., Maraschi L., 1991, 380, L51

Holt S. S., Mushotzky R. F., Boldt E. A., Serlemitsos P. J., Becker R. H., Szymkowiak A. E., White N. E., 1980, ApJL, 241, L13

Magdziarz, P., Zdziarski, A. A., 1995, MNRAS, 273, 837.

Morrison R., McCammon D., 1983, ApJ, 270, 119

Ogle P. M., Marshall H. L., Lee J. C., Canizares C. R., 2000, ApJL, 545, L81

Petrucci P. O., Haardt F., Maraschi L., Grandi P., Matt G., Nicastro F., Piro L., Perola G. C., De Rosa A., 2000, ApJ, 540, 131

Schurch N. J., Warwick R., 2002, MNRAS, submitted.

Strüder, L., Briel, U., Dennerl, K. et al. 2001, A&A, 365.

Turner, M.J.L., Abbey, A.F., Arnaud, M. et al. 2001, A&A, 365.

Wang J., Wang T., Zhou Y., 2001, ApJ, 549, 891

Weaver K. A., Mushotzky R. F., Arnaud K. A., Serlemitsos P. J., Marshall F. E., Petre R., Jahoda K. M., Smale A. P., Netzer H., 1994a, ApJ, 423, 621

Weaver K. A., Yaqoob T., Holt S. S., Mushotzky R. F., Matsuoka M., Yamauchi M., 1994b, APJL, 436, L27

Yaqoob T., Warwick R. S., 1991, MNRAS, 248, 773

Yaqoob T., Warwick R. S., Makino F., Otani C., Sokoloski J. L., Bond I. A., Yamauchi M., 1993, MNRAS, 262, 435

Yaqoob T., Edelson R., Weaver K. A., Warwick R. S., Mushotzky R. F., Serlemitsos P. J., Holt S. S, 1995, ApJL, 453, L81

Zdziarski A. A., Fabian A. C., Nandra K., Celotti A., Rees M. J., Done C., Coppi P. S., Madejski G. M., 1994, MNRAS, 269, L55

Zdziarski A. A., Johnson W. N., Magdziarz P. 1996, MNRAS, 283, 193

Zdziarski A. A., Poutanen J., Johnson W. N., 2000, ApJ, 542, 703